AIP | Applied Physics Letters

Phase and dielectric behaviors of a polymorphic liquid crystal doped with graphene nanoplatelets

Po-Chang Wu and Wei Lee

Citation: Applied Physics Letters **102**, 162904 (2013); doi: 10.1063/1.4802839
View online: http://dx.doi.org/10.1063/1.4802839
View Table of Contents: http://scitation.aip.org/content/aip/journal/apl/102/16?ver=pdfcov
Published by the AIP Publishing

Phase and dielectric behaviors of a polymorphic liquid crystal doped with graphene nanoplatelets

Po-Chang Wu and Wei Lee[a)]
College of Photonics, National Chiao Tung University, Guiren, Tainan 71150, Taiwan

(Received 17 March 2013; accepted 7 April 2013; published online 24 April 2013)

We report on the phase behavior and dielectric properties of the liquid crystal (LC) 4′-*n*-octyloxy-4-cyanobiphenyl dispersed with graphene nanoplatelets (GNPs). The temperature-dependent dielectric permittivity at 10^4 Hz and its derivative with respect to the temperature reveal that the incorporation of GNPs in a LC cell leads to the modification of crystalline polymorphism and shift in phase transition temperature owing to the enhanced positional and orientational order. Additionally, the dielectric data between 1 and 10^3 Hz show that the dopant reduces the ionic concentration and alters the diffusivity in the LC mesophases. © *2013 AIP Publishing LLC* [http://dx.doi.org/10.1063/1.4802839]

Colloids of nanoscale materials dispersed in liquid crystals (LCs) have been a subject of extensive research during the last decade. From the point of view of practical applications, manipulation of the physical properties of existing LCs by doping with various types of nanomaterials has been evidenced for the improvement of electro-optical performance in LC devices.[1,2] Moreover, investigations demonstrating the suppressed ionic effect by nanodopants have also been clarified for solving image problems in LC displays caused by ubiquitous impurity ions.[3–7] Depending on the intrinsic characteristics of the dopant and mutual interaction with LC molecules, researchers have studied the individual effects of nanomaterial additives on the behaviors of phase transitions in LCs in terms of the molecular ordering,[8,9] dielectric relaxation,[10] and electrophysical properties of LCs.[11–13]

Among currently available nanomaterials, graphene, classified as a two-dimensional (2-D) carbon allotrope, has attracted immense attention for potential applications in electronic devices and nanocomposites since its successful isolation in 2004.[14] An alluring feature of graphene for optoelectronic uses is its high transparency and high conductivity, suitable for replacing indium–tin oxide (ITO) as an alternative electrode material.[15] As the interest in LC suspensions grows readily in current nanoscience, researchers have investigated the optical manipulation in a LC/graphene nanostructure[16] as well as applications of graphene in cholesteric[17] and polymer-dispersed[18] LCs very recently.

In the present work, we consider several colloidal suspensions of polymorphic LC impregnated with various contents of graphene nanoplatelets (GNPs) and look into the phase behavior and ionic properties of the hybrids based on temperature-dependent dielectric spectroscopy and polarizing optical microscopy. Our observations reveal that the process of crystallization in the solid phase, the order of LC molecules, and the transition temperature between two adjacent phases are all significantly influenced by the GNP dopant. In addition, the dielectric spectra in the low-frequency regime ($f \leq 1$ kHz), characterized by space-charge polarization, allow one to investigate the impurity-ion properties of GNP-doped LC cells in comparison with their neat counterpart. The data manifest the reduced ionic concentration and modified diffusivity.

The LC host used in this study was 4-*n*-octyloxy-4′-cyanobiphenyl (8OCB), a polar single compound exhibiting polymorphism with the following phase transition sequence: Crystal (Cr)–55 °C–Smectic A (SmA)–67 °C–Nematic (N)–80 °C–Isotropic (I). The GNP (xGNP-05), purchased from XG Sciences, contains more than 16 graphene layers with an average thickness of 10 nm and diameter of 5 μm. In order to promote homogeneity and uniform dispersion, the GNPs as received were first baked in a vacuum oven at 150 °C for 6 h to evaporate residual moistures, followed by ball milling for disaggregation and reduction in size. The condition of ball milling was optimized based on our previous work.[3] The sizes of GNPs were reduced to the order of sub-micrometers. Various 8OCB/GNP mixtures were prepared with GNP concentrations ranging from 0.03 to 0.50 wt. %, as determined by a Mettler Toledo X26 analytical balance. All mixtures were put in an ultrasonic bath for 2 h and then stirred for 1 h. By capillary action at 70 °C where the LC was in the N phase, pristine 8OCB and the well-dispersed colloids were individually introduced into glass cells, each composed of a pair of ITO-coated glass substrates covered with planar alignment films. The cell gap was 7.0 ± 0.5 μm. Temperature-dependent dielectric spectra in the frequency range of 1 Hz–100 kHz were acquired with a high-precision LCR meter (HIOKI 3522-50). The probe voltage for the dielectric measurement was 0.1 V in the sinusoidal waveform; this amplitude was smaller than the threshold voltage of 8OCB. The dielectric data were obtained in the temperature range controlled between 30 and 90 °C with an accuracy of ±0.5 °C.

The complex dielectric function $\varepsilon^* = \varepsilon' - i\varepsilon''$ depends generally on the frequency (f) and temperature (T). In the frequency regime between 10^3 and 10^5 Hz, the real part ε', dictated by the orientation of 8OCB molecules, exhibits no dependence on f. Because of the strong T dependence of molecular ordering, the variation of ε' with T in this frequency regime can be used to clarify the phase behavior and thermal

[a)]Electronic mail: wlee@nctu.edu.tw.

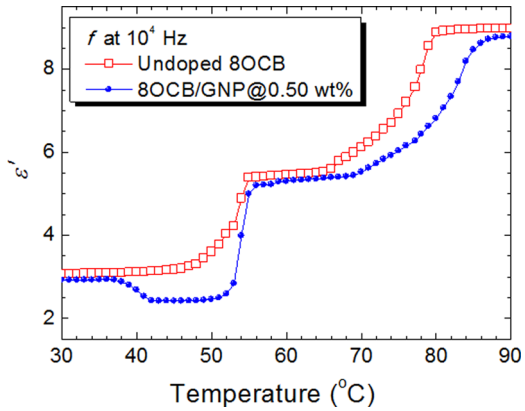

FIG. 1. Real-part dielectric constant of pure and GNP-doped 8OCB cells at 10^4 Hz as a function of the temperature at the rate of 1 °C/min. The dopant concentration for the doped cell is 0.50 wt. %.

stability of LC molecules.[19,20] Moreover, the derivative of ε' with respect to T, $d\varepsilon'/dT$, is a sensitive probe for determining the phase transition.[20,21] Figure 1 shows the temperature dependence of the real-part dielectric function $\varepsilon'(T)$ of a pure cell and a doped cell containing 0.50 wt. % GNPs at 10^4 Hz. Starting from the crystalline phase in the case of pristine 8OCB, $\varepsilon'(T)$ increases with rising T from 45 to 55 °C until it reaches the SmA phase where $\varepsilon'(T)$ remains constant. This result is regarded as the pre-transitional behavior between the solid and LC states attributed to the increased kinetic energy of the molecules. Further raising T above the SmA-to-N phase transition point (~67 °C) causes the increase in $\varepsilon'(T)$ due to the thermal-induced reduction in LC molecular order in the N phase. The value of $\varepsilon'(T)$ further reaches a stable level at high temperatures (>80 °C) in the I phase. Compared with that of the pure counterpart, $\varepsilon'(T)$ of the GNP-doped cell varies similarly in the SmA, N, and I phases. Notably, the values of $\varepsilon'(T)$ for the doped sample are much lower especially at the temperatures covering the N phase. In the planar-aligned LC cell, ε' corresponds to the perpendicular component $\varepsilon_\perp$ of the LC phases. Since the increase in ε' with increasing temperature is expected for the LC 8OCB with positive dielectric anisotropy, the lowered value of ε' in the N phase of GNP-doped LC cell indicates less variation of molecular ordering with temperature. This result implies that the presence of GNPs induces the reinforced structural order. In view of the intermolecular interaction between LC and carbon nanotubes (CNTs)[8] and the superior mechanical and thermal properties of GNPs, it can be deemed that the coupling between the basal plane of GNP and LC creates an in-plane anchoring force to the LC molecules and thus enhances the molecular order as well as its thermal stability. When the phase transforms from SmA to N, the 2-D layered structure of GNPs serves to consolidate the smectic layers, spatially maintaining the molecular orientation. Figure 1 also presents an abrupt drop of $\varepsilon'(T)$ between 37 and 42 °C in the crystalline phase of the GNP-doped sample. This result is distinct from the neat 8OCB cell in which $\varepsilon'(T)$ retains almost unchanged until T reaches the Cr–SmA pre-transition point. The drop implies that there is an additional Cr-to-Cr phase transition in the doped cell. Further examination of microscopic textures indicates that only the most stable powder-crystalline form (CrA) with perfect single domain can be observed within the crystalline phase of pure 8OCB as shown in Fig. 2(a). By contrast, poly-domain crystalline form (CrB) is exhibited in the GNP-doped cell at 30 °C (Fig. 2(b)). As the temperature increases to a specific value near 40 °C, a transformation from CrB to the more stable crystal form CrC takes place via the nucleation of crystal domains. As a matter of fact, CrB is a metastable form, spontaneously turning to the stable CrC form in several days at room temperature. The CrB-to-CrC transition temperature $T_{CrB–CrC}$ in GNP-doped cells is dependent of the GNP concentration. In the case of the 0.50 wt. % content, $T_{CrB–CrC}$ is about 40 °C as depicted in Fig. 2(b). Note that the appearances of the CrA and CrC forms are both opaque-white whereas the CrB form appears transparent. In 8OCB polymorphism, four crystalline forms—one stable state and three metastable states—have been observed by various methods.[22,23] In GNP-doped cells, we observed that the CrB form is generated by the expansion of platelet-like domains originating from the GNPs during the cooling process in the solid phase. It is explained that the enhanced order gradually declines as the LC molecules are

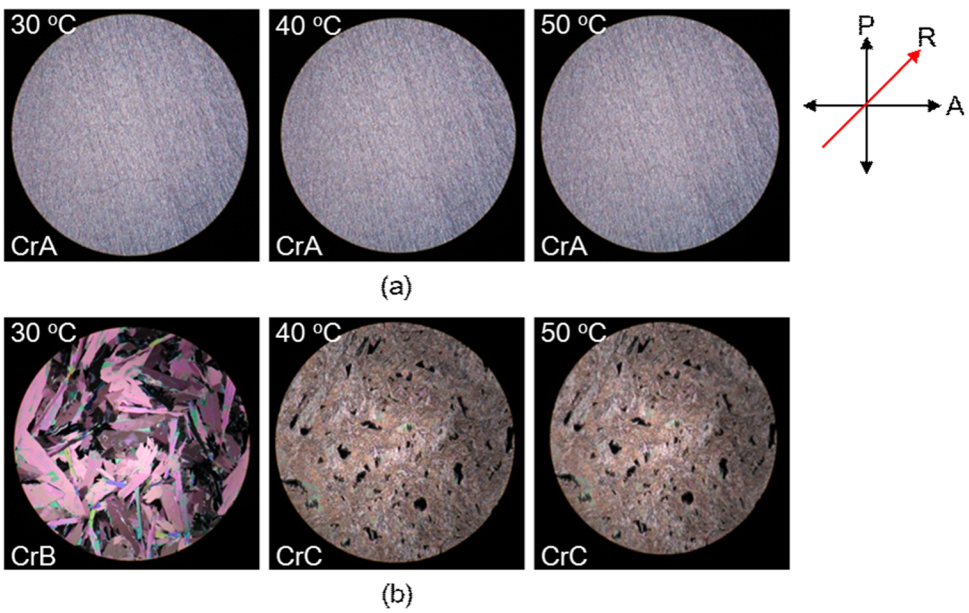

FIG. 2. Microscopic textures of (a) pure and (b) 0.50 wt. % GNP-doped 8OCB cells in the crystalline phase at different temperatures. Here, P, A, and R represent the transmission axes of the polarizer, analyzer, and the rubbing direction, respectively.

aligned farther away from the GNPs. In other words, the dispersed GNPs serve as the nuclei, causing the change in energy for the LC molecules surrounding the GNPs during the crystallization process. The breaking in symmetry of molecular ordering by the scattered GNPs thus hinders the crystallization into the single-domain form CrA and gives rise to the poly-domain CrB form.

The phase transition temperatures of the undoped and doped cells can be discussed more explicitly in terms of $d\varepsilon'/dT$ as a function of the temperature as shown in Fig. 3. Figure 3(a) exhibits three peaks at 54, 67, and 78 °C in the case of the pure 8OCB cell. These values are quite consistent with the known $T_{Cr–SmA}$, $T_{SmA–N}$, and $T_{N–I}$, respectively, in accordance with the phase diagram of the pure 8OCB. Doping GNPs in 8OCB results in an additional feature—upside-down peak—corresponding to the CrB–CrC phase transition. Depending on c, the temperature for this upside-down peak is located around 40 to 44 °C as illustrated in Figs. 3(b)–3(f). One can see that $T_{CrB–CrC}$ decreases with increasing c, presumably due to the domain-size dependence of transition energy. Since the dispersed GNPs are nuclei of these platelet domains, more GNPs contained in the cell are considered to create smaller domain sizes in the restricted cell space. Once the T is elevated (>30 °C), 8OCB molecules in the CrB form characterized by numerous smaller domains can transform to CrC much more easily. Obviously, Fig. 3 also reveals the shifts of both $T_{SmA–N}$ and $T_{N–I}$ to higher temperatures as c goes beyond 0.10 wt. %. The extension of $T_{N–I}$ can be referred to as the enhanced orientational order by GNPs which has also been observed in LC/CNT dispersions.[11] Figure 4 summarizes the phase transition temperatures deduced from Fig. 3. It is obvious that $T_{CrB–CrC}$, $T_{SmA–N}$, and $T_{N–I}$ are modified from 44 to 40 °C, 67 to 71 °C, and 78 to 83 °C, respectively, as c is increased up to 0.50 wt. %.

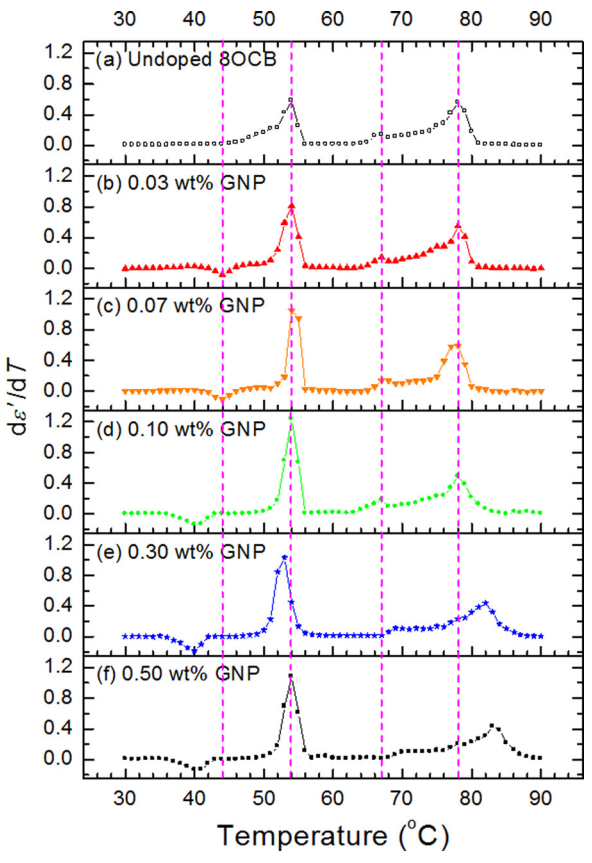

FIG. 3. The first-order derivative of the real-part dielectric constant with respect to temperature of various 8OCB cells.

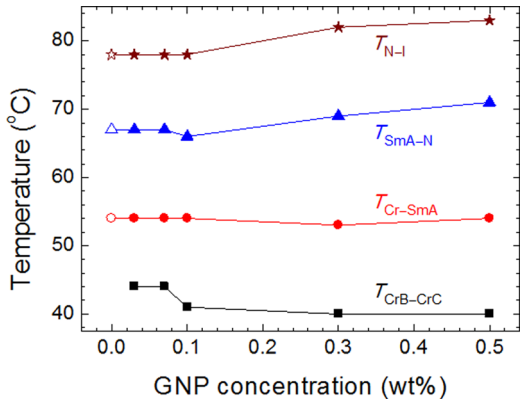

FIG. 4. Phase transition temperatures of undoped and doped 8OCB cells with different GNP concentrations.

In regard to the dielectric response in the frequency range between 1 and 10^3 Hz, the complex dielectric function is characterized by the motion of mobile ions in which ε' and ε'' are inversely proportional to $f^{-3/2}$ and f^{-1}, respectively. Because of the large scatter in the dielectric data for the solid phase, the T-dependent ionic properties were investigated within the temperature range from 60 to 90 °C, covering the SmA to I phases of 8OCB. Following the model established by Uemura,[24,25] the complex dielectric function can be written as

$$\varepsilon'(f) = \frac{2nq^2D^{\frac{3}{2}}}{\varepsilon_0\sqrt{\pi}dk_BT}f^{-\frac{3}{2}} \quad (1)$$

and

$$\varepsilon''(f) = \frac{2nq^2D}{\varepsilon_0 k_BT}f^{-1}, \quad (2)$$

where n is the ionic concentration, q is the electric charge, D is the diffusivity of the ions, d is the cell gap, ε_0 is the permittivity in free space, k_B is the Boltzmann constant, and T is the absolute temperature. Consequentially, n and D can be obtained by fitting the experimental data of ε' and ε'' according to Eqs. (1) and (2). Figure 5(a) shows the fitted ionic concentrations in undoped and doped 8OCB cells. Noticeably, n in either phase is nearly invariant to T for each cell. Such a T-independent ionic concentration has been reported in the N phase and explained by the absence of the ionic association–dissociation reaction.[3] Here, the approximately invariant n in the individual SmA and N phases is attributable to the similar molecular orientation across the continuous (namely, second-order) phase transition. As T increases, n drops steeply just near the N–I phase transition temperature on account of the dipole interaction between the polar LC molecules rather than the dopant effect. Clearly from Fig. 5(a), all GNP-doped cells exhibit lower n in the entire temperature range, indicating that the dispersion of GNPs is responsible for trapping mobile impurity ions. For the 0.50 wt. % dopant content, the value of n is reduced, from 2.5 to 1.7×10^{12} cm^{-3}, by 30%.

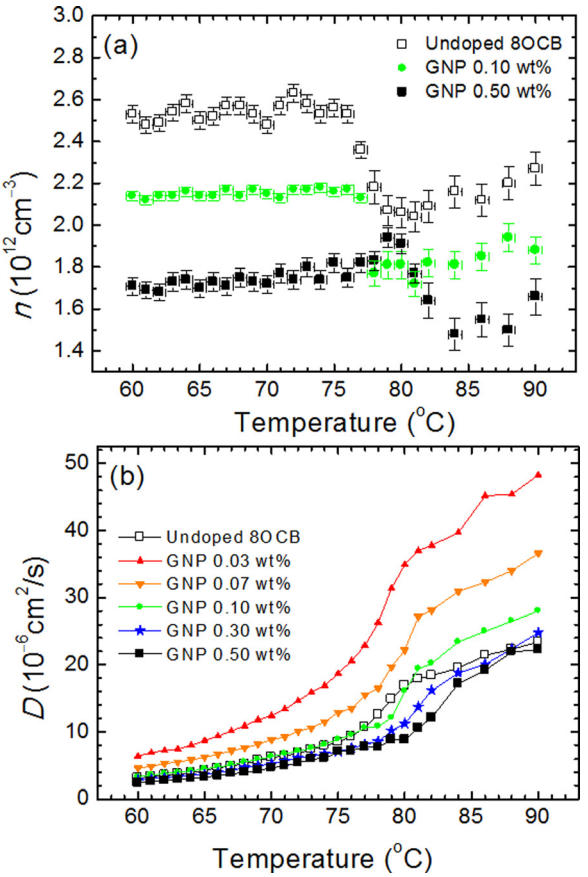

FIG. 5. Temperature-dependent (a) ionic concentrations and (b) diffusivities in various 8OCB cells.

Figure 5(b) presents the temperature-dependent diffusivities in the pure and doped 8OCB. For all cells, $D(T)$ increases with increasing T. In the doped cells with GNP contents of 0.03 and 0.07 wt. %, D is higher than that in the undoped cell in the entire temperature range. At these two dopant concentrations, the effect of GNPs on the molecular order is very weak since the phase transition temperatures of both SmA–N and N–I are identical to those of the pristine counterpart as displayed in Fig. 3. In consideration of the dimensions of GNPs used in this study, the distributed GNPs in a 7 μm-thick cell are likely to form percolated networks and, in turn, lead to the increase in diffusivity and electrical conductivity as well. On the other hand, D is lowered as c increases beyond 0.10 wt. %, indicating the remarkable ability of hindering the ion transport. It is known that GNPs tend to conglomerate at higher concentrations, increasing the viscosity of LC colloids.[18] In this study, the lowered D seems to stem from the increasing flow viscosity, speculatively due to the pronounced enhancement of the molecular order by GNPs. With the limited variation in ionic concentration, the behavior of the temperature-varying dc conductivity is primarily governed by the ionic diffusivity.

In summary, temperature-dependent dielectric properties of the polymorphic LC 8OCB doped with GNPs are investigated by dielectric spectroscopy. Our results indicate that, different from the conventional methods for obtaining metastable crystalline forms, a metastable poly-domain crystalline form (CrB) can readily be generated in the solid phase for GNP-doped samples owing to the presence of the dopant serving as nuclei during crystallization. The transformation from the metastable crystalline form to the more stable crystallize form (CrC) is achieved in the temperature-heating process. The transition temperature between these crystalline forms decreases with increasing dopant concentration. With the first derivative of $\varepsilon'(T)$, this study demonstrates that T_{SmA-N} and T_{N-I} shift to higher temperatures by 4 and 5 °C, respectively, as the dopant concentration increases from 0.03 to 0.50 wt. % due to the elevated positional and orientational order. By means of Eqs. (1) and (2), the temperature-dependent ion concentration and diffusivity are deduced for various cells using the dielectric data in the low-frequency regime ($f \leq 10^3$ Hz). Experimental results reveal that the GNPs as a dopant possess the ability to trap impurity ions, with efficacy to be of temperature independence. Our results also suggest that the diffusivity can be reduced when the dopant concentration is high enough ($c = 0.30$ or 0.50 wt. %) to presumably enhance the molecular order and increase the viscosity.

The authors thank Professor Victor Ya. Zyryanov of Kirensky Institute of Physics, Siberian Branch of the Russian Academy of Sciences for providing 8OCB. This work was financially supported by the National Science Council of the Republic of China (Taiwan) through Grant Nos. NSC 101-2112-M-009-018-MY3 and NSC 101-2811-M-009-059.

[1]H. Qi and T. Hegmann, J. Mater. Chem. **18**, 3288 (2008).
[2]H. K. Bisoyi and S. Kumar, Chem. Soc. Rev. **40**, 306 (2011).
[3]B.-R. Jian, C.-Y. Tang, and W. Lee, Carbon **49**, 910 (2011).
[4]H.-H. Liu and W. Lee, Appl. Phys. Lett. **97**, 023510 (2010).
[5]H.-H. Liu and W. Lee, Appl. Phys. Lett. **97**, 173501 (2010).
[6]C.-Y. Tang, S.-M. Huang, and W. Lee, J. Phys. D: Appl. Phys. **44**, 355102 (2011).
[7]S.-W. Liao, C.-T. Hsieh, C.-C. Kuo, and C.-Y. Huang, Appl. Phys. Lett. **101**, 161906 (2012).
[8]R. Basu and G. S. Iannacchione, Appl. Phys. Lett. **95**, 173113 (2009).
[9]C. D. Cruz, O. Sandre, and V. Cabuil, J. Phys. Chem. B **109**, 14292 (2005).
[10]A. Malik, A. Choudhary, P. Silotia, and A. M. Biradar, J. Appl. Phys. **110**, 064111 (2011).
[11]N. Lebovka, T. Dadakova, L. Lysetskiy, O. Melezhyk, G. Puchkovska, T. Gavrilko, J. Baran, and M. Drozd, J. Mol. Struct. **887**, 135 (2008).
[12]A. I. Goncharuk, N. I. Lebovka, L. N. Lisetski, and S. S. Minenko, J. Phys. D: Appl. Phys. **42**, 165411 (2009).
[13]L. N. Lisetski, S. S. Minenko, V. V. Ponevchinsky, M. S. Soskin, A. I. Goncharuk, and N. I. Lebovka, Materialwiss. Werkstofftech. **42**, 5 (2011).
[14]K. S. Novoselov, A. K. Geim, S. V. MorozovK, S. Novoselov, S. V. Morozov, D. Jiang, Y. Zhang, S. V. Dubonos, I. V. Grigorieva, and A. A. Firsov, Science **306**, 666 (2004).
[15]P. Blake, P. D. Brimicombe, R. R. Nair, T. J. Booth, D. Jiang, F. Schedin, L. A. Ponomarenko, S. V. Morozov, H. F. Gleeson, E. W. Hill, A. K. Geim, and K. S. Novoselov, Nano Lett. **8**, 1704 (2008).
[16]C. W. Twombly, J. S. Evans, and I. Smalyukh, Opt. Express **21**, 1324 (2013).
[17]Z. Xu and C. Gao, Nature Commun. **2**, 571 (2011).
[18]B. K. Kim, M. W. Jang, H. C. Park, H. M. Jeong, and E. Y. Kim, J. Polym. Sci. Part A: Polym. Chem. **50**, 1418 (2012).
[19]M. Marik, M. Rahman, B. K. Chaudhuri, and A. Yoshizawa, Phase Transitions **85**, 201 (2012).
[20]G. Grigoriadis, H. Duran, M. Steinhart, M. Kappl, H. J. Butt, and G. Floudas, ACS Nano **5**, 9208 (2011).
[21]P. Cusmin, M. R. de la Fuente, J. Salud, M. A. Perez-Jubindo, S. Diez-Berart, and D. O. Lopez, J. Phys. Chem. B **111**, 8974 (2007).
[22]K. Horu and H. Wu, Liq. Cryst. **26**, 37 (1999).
[23]A. Jákli, I. Jánossy, and A. Vajda, Liq. Cryst. **27**, 1035 (2000).
[24]S. Uemura, J. Polym. Sci. A **10**, 2155 (1972).
[25]S. Uemura, J. Polym. Sci., Polym. Phys. Ed. **12**, 1177 (1974).